Electronic structures and magnetic properties of Fe_2P and the effects of doping with Ni

1993 J. Phys.: Condens. Matter 5 9307

(http://iopscience.iop.org/0953-8984/5/50/012)

J. Phys.: Condens. Matter 5 (1993) 9307–9316. Printed in the UK

Electronic structures and magnetic properties of Fe_2P and the effects of doping with Ni

Cai Jian-Wang†, Luo He-Lie† and Zheng Qing-Qi‡

† State Key Laboratory of Magnetism, Institute of Physics, Academia Sinica, Beijing 100 080, People's Republic of China

‡ Institute of Solid State Physics, Academia Sinica, Hefei 230031, People's Republic of China

Received 12 July 1993, in final form 13 September 1993

Abstract. The first-principles self-consistent cluster method has been used to study the electronic structures and magnetic properties of Fe_2P and the effect of doping with Ni. We find that, for Fe_2P, the local magnetic moments of Fe_I atoms at the tetrahedral sites are smaller than those of Fe_{II} atoms at the pyramidal sites owing to the greater hybridization of Fe_I with P; when Ni atoms replace Fe_I atoms, the Fe_{II} magnetic moment shows a slight increase and the ferromagnetism of the $(Fe_{1-x}Ni_x)_2P$ compounds is strengthened. However, the substitutions of Ni in Fe_{II} sites reduce the Fe_I atom magnetic moment substantially. These results are in good agreement with experiments.

1. Introduction

For many years, the Fe–P system and other transition-metal–metalloid systems have been subjected to intense experimental and theoretical investigations. This is not only because these transition-metal–metalloid systems have vast applications owing to their special mechanical, electromechanical and magnetic properties, but also because the physics and chemistry of these materials are highly interesting. The Fe–P system forms the BCC structure when the P content is less than 12% [1]. Above this concentration, the amorphous phases as well as various crystalline compounds prevail [2–4]. Among these crystalline phases, the compound Fe_2P has attracted much interest, and its magnetic properties have been extensively studied by various experimental techniques, e.g. magnetization measurement, Mössbauer spectroscopy and neutron scattering [5–7].

Fe_2P is a ferromagnet with a Curie temperature $T_C = 209$ K, accompanied by a first-order transition, and has an unusually large magnetocrystalline anisotropy K_1 of 2.32×10^7 erg cm^{-3} [5]. From the hyperfine field at 15 K [6], the magnetic moments were deduced to be 1.14 μ_B and 1.78 μ_B for Fe_I atoms at tetrahedral sites and Fe_{II} atoms at pyramidal sites, respectively, while the polarized neutron diffraction experiment at 77 K [7] revealed that the magnetic moments of Fe_I and Fe_{II} atoms are 0.92 μ_B and 1.70 μ_B, respectively. An interesting aspect of the magnetic properties of Fe_2P is its magnetic behaviour when doped with other transition metals [8–13]. Substitutions of small amounts of Mn or Cr destroy the ferromagnetism, lead to antiferromagnetism, and also reduce the ordering temperature; the hyperfine fields at the two Fe sites are drastically reduced. Co and Ni, on the other hand, when substituted for Fe, raise the ordering temperature and thus strengthen the ferromagnetism. Studies of $(Fe_{1-x}Ni_x)_2P$ compounds [12, 13] have shown that the Curie temperature has a maximum at about $x = 0.1$ while the anisotropy constant

0953-8984/93/509307+10$07.50

K_1 decreases rapidly with increasing x and becomes almost zero near $x = 0.3$. The Fe magnetic moments hardly change in the range $x < 0.3$ and decrease with increasing x for $x > 0.3$.

In contrast with the abundant experimental data, there seems to be hardly any theoretical study on the local magnetic properties of Fe_2P and the magnetic behaviour of transition-metal-substituted Fe_2P. Although considerable theoretical work has been done to investigate the magnetic properties of transition-metal–metalloid systems, these results cannot offer a satisfying answer to the problem of Fe_2P [14, 15]. The purpose of this paper is to calculate the different local magnetic moments and densities of states (DOSs) of Fe atoms with various local environments and to give a theoretical description of the magnetic properties of Fe_2P and the effects of doping with Ni. For transition metals and intermetallic compounds, it is now well recognized that the local magnetic properties and electronic structures are mostly determined by the local environments of atoms. In this paper, we use embedded clusters to simulate the local environment of Fe atoms for Fe_2P and Ni-substituted Fe_2P and perform first-principles electronic structure calculations on these clusters within the framework of the discrete variational method (DVM), which has been shown to be highly successful in describing the properties of transition metals and intermetallic compounds [16–19].

The paper is organized as follows. We briefly describe the cluster model and the outline of the theoretical approach in section 2. Our results are presented and discussed in section 3. A summary of our conclusions is contained in section 4.

2. Cluster model and theoretical approach

Fe_2P has a hexagonal structure, which belongs to the C_{22} type and the space group is $P\bar{6}2m$ (D^3_{3h}). The system $(Fe_{1-x}Ni_x)_2P$ has complete solid solutions with this hexagonal structure [8]. In this structure, P atoms form a channel aligned along the c axis, and there are two M-atom sites (M≡Fe or Ni). One of them, M_I is surrounded by four P atoms which form a nearly cubic tetrahedron and the other M atom, M_{II}, is surrounded by five P atoms which form a pyramid (figure 1). There are considerable differences between M_I and M_{II} atoms in the environment of the near-neighbour atoms. On the basis of all the above, the 33-atom cluster, which contains six M_I atoms, 12 M_{II} atoms and 15 P atoms with D_{3h} symmetry (figure 2), is chosen to represent these hexagonal compounds.

The electronic structures of the clusters are obtained by using a linear-combination-of-atomic-orbitals DVM, within the framework of the density-functional theory and the local-spin-density approximation, which have been described in detail elsewhere [20].

The non-relativistic one-electron Hamiltonian for a cluster of atoms in the self-consistent spin-polarized local-density formalism is given in Hartree atomic units by

$$h_\sigma = -\tfrac{1}{2}\nabla^2 + V_{\mathrm{Coul}}(\rho_\sigma) + V_{\mathrm{xc}}(\rho_\sigma).$$

The Coulomb potential $V_{\mathrm{Coul}}(\rho_\sigma)$ includes both electron–electron and electron–nuclei interactions. The local potential $V_{\mathrm{xc}}(\rho_\sigma)$ for exchange–correlation is chosen to be of the spin-polarized von Barth–Hedin [21] form. The electron density $\rho_\sigma(r)$ for each spin is expressed as a sum over molecular spin orbitals $\Phi_{i\sigma}(r)$ with occupation $n_{i\sigma}$:

$$\rho_\sigma(r) = \sum_i n_{i\sigma} |\Phi_{i\sigma}(r)|^2$$

where the molecular spin orbitals $\Phi_{i\sigma}$ are expanded in terms of symmetrized atomic orbitals, which are chosen as linear combinations of atomic orbitals centred on different atoms corresponding to the cluster point group symmetry.

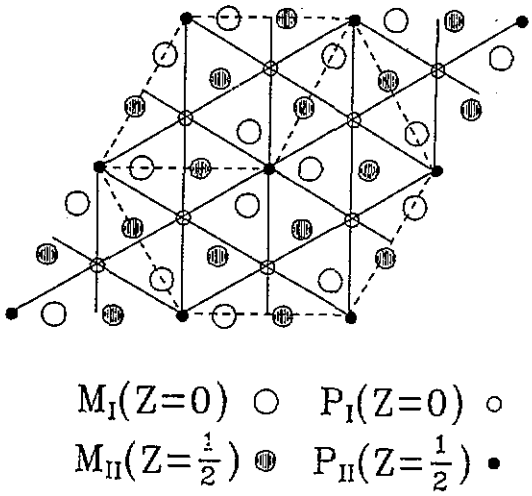

Figure 1. Arrangement of rhombohedral subcells in the hexagonal Fe_2P structure.

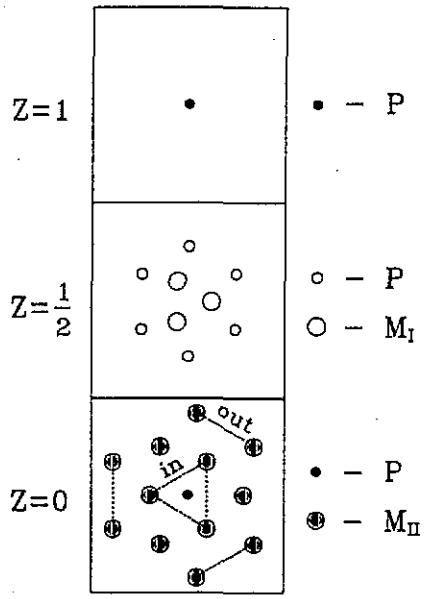

Figure 2. Upper portion of 33-atom cluster representing the hexagonal M_2P system.

The atomic basis set of the form $R_{nl}Y_{lm}(\theta,\varphi)$, where $R_{nl}(r)$ are numerical radial functions, are obtained from density-functional calculations. Spherical potential wells around the Fe and P atoms are employed to compress diffuse valence orbitals and thus to control the linear dependence of the basis set. In the variational expansion of the cluster spin orbitals $\Phi_{i\sigma}(r)$, the frozen-core approximation is used; the numerical atomic orbitals 3d, 4s and 4p for Fe and 3s and 3p for P, are kept in the variational basis.

Then the secular equations $(\mathbf{H}-E\mathbf{S})C=\mathbf{0}$ are solved self-consistently using matrix elements determined by three-dimensional numerical integrations performed on a random-point grid by the diophantine method [20]. About 500 sampling points per atom are found to be sufficient for convergence in the DOS and the eigenvalue spectrum to within 0.01 eV. In constructing the cluster potential, we adopt the so-called self-consistent-charge (SCC) approximation, i.e. the actual electronic density is fitted to a model variational charge density $\rho_\sigma^{SCC}(r)$, which is a superposition of radial densities R_{nl}^ν centred on cluster atoms via the diagonal-weighted Mulliken population f_{nl}^ν:

$$\rho_\sigma^{SCC}=\sum_{nl}\sum_{\nu}f_{nl}^{\nu}|R_{nl}(r_\nu)|^2.$$

The coefficients f_{nl}^ν are determined variationally in each cycle; they determine the cluster potential in the next cycle. Repeatedly, self-consistency is achieved through convergence of these Mulliken populations.

In order to diminish spurious effects of simulating the solid by a cluster of atoms, all clusters are surrounded by several shells of atoms of the Fe_2P microcrystal. The embedding potentials are derived from superposition of charge density placed at these crystal sites exterior to the cluster. The charge density of the exterior atoms is obtained by taking the effective atomic configurations and the known experimental moments. Localization of cluster orbitals due to the Pauli exclusion principle is simulated by truncation at the

core region of the potential of the exterior atoms. The results are greatly improved by the embedding scheme, which has been widely employed.

Local-spin-density self-consistent field models of electronic structure have proved to be highly successful in describing the properties of transition metals and intermetallic compounds. For a periodic system, the cluster model tends to the same limit as band-structure methods when the cluster size increases. In treating alloy properties or impurities in transition metals, representation of the system by a small embedded cluster is not only computationally attractive but also physically reasonable.

3. Results and discussion

3.1. Fe_2P

In table 1, we give the local magnetic moments and the electron occupation numbers of atoms in the cluster $Fe_3Fe_3Fe_6Fe_6P_1P_{12}P_2$ representing Fe_2P. It is noticed that all Fe atoms are ferromagnetically coupled with large positive magnetic moments, and that P atoms are negatively polarized with small values. These results show that the ground state of Fe_2P is ferromagnetic.

Analysing table 1, one can find that the outer Fe atoms, with moments 4.51 μ_B and 3d, 4s and 4p with electron numbers 6.03, 1.17 and 0.69, respectively, show a surface-like behaviour and deviate from the properties of the bulk solid greatly, while the inner three Fe atoms on the $z = 0$ plane and the six Fe atoms on the $z = \pm\frac{1}{2}$ plane have moments of 2.12 μ_B and 1.59 μ_B respectively, which approach the experimental values of pyramidal and tetrahedral Fe atoms in Fe_2P. For each Fe site of the cluster, in table 1, we also give its number of P and Fe neighbours. Clearly, the outer Fe atoms have incomplete neighbour shells, while the inner Fe atoms have similar local environments to Fe_{II} and Fe_I sites in bulk Fe_2P, which are surrounded by five and four P atoms, respectively. The inner atoms show the most bulk-like properties; so they were chosen for evaluation of the properties of Fe_{II} and Fe_I sites in Fe_2P.

Comparing the calculated magnetic moments with the experimental values, we can see that the calculated value is somewhat larger than the experimental result owing to the finite-cluster-size effect because the overlap of orbital wavefunctions in the cluster is not so complete as that in the bulk solid. The convergence of the magnetic moment to a bulk value has been studied by Press *et al* [22], who showed that the magnetic moment of the central atom in a cluster of 43 Ni-atoms can reproduce the bulk value very well. The chosen 33-atom cluster seems to be not large enough to reproduce magnetic moments of Fe_2P; however, it predicts that the moment of pyramidal Fe atoms is much larger than that of tetrahedral Fe atoms. A cluster with one or two more shells can reduce the magnetic moment and make it closer to the experimental value but, accordingly, it is much more expensive to compute. Many calculations on metal clusters have shown that a cluster with three- to four-atom shells is sufficient to describe most physical properties of the metal and, for its magnetic moments, one can focus preferably on the trend rather than the absolute value. From this point of view, our calculated moment is in good agreement with the experimental results [6, 7].

From the electron occupation numbers of cluster atoms, which are also listed in table 1, we can see that there are no substantial charge transfers to or from P to Fe, and the 3d occupations are nearly the same for Fe_I and Fe_{II} atoms, which shows that the difference between the moments of the Fe_I and Fe_{II} atoms cannot result from their different d occupations.

Table 1. Local magnetic moments μ_i and electron occupation numbers n_i of different sites in the cluster $Fe_3Fe_3Fe_6Fe_6P_1P_{12}P_2$ representing Fe_2P.

Site	Atoms in Cluster	Position	μ_{3d} (μ_B)	μ_{4s+4p} (μ_B)	μ_{total} (μ_B)	n_{3d}	n_{4s}	n_{4p}	n_{3s+3p}	Number of P neighbours	Number of Fe neighbours
Pyramidal	Fe_3	$z = 0$ (in) Fe_{II}	2.06	0.06	2.12	6.34	0.60	0.74		5	$4Fe_I + 4Fe_{II}$
Pyramidal	Fe_3	$z = 0$ (mediate)	3.04	0.27	3.31	6.15	0.82	0.93		4	$4Fe_{II}$
Pyramidal	Fe_6	$z = 0$ (out)	3.82	0.69	4.51	6.03	1.17	0.69		2	$2Fe_{II}$
Tetrahedral	Fe_6	$z = \pm\frac{1}{2}$ Fe_I	1.54	0.05	1.59	6.32	0.59	0.82		4	$2Fe_I + 3Fe_{II}$
	P_1	$z = 0$			−0.19				5.13		
	P_{12}	$z = \pm\frac{1}{2}$			−0.25				5.23		
	P_2	$z = \pm 1$			−0.25				5.31		

Knowledge of the crystal structures of Fe_2P [23] tells us that an Fe_{II} is surrounded by five P atoms which are at distances of 2.38 and 2.48 Å from an Fe_{II} atom; however, an Fe_I atom is surrounded by four P atoms which are at distances of 2.22 and 2.29 Å. So the interaction between Fe_I and P atoms is much stronger than that between Fe_{II} and P atoms. In figure 3, we show the charge density on the $z = 0$ and $z = \frac{1}{2}$ planes. It can be seen that there is hardly any overlap of charge density between Fe_{II} and P atoms (figure 3(*a*)) while the charge density spatially extends over the Fe_I and P atoms (figure 3(*b*)). Therefore, the influence of P on Fe_{II} is less than that on Fe_I; this results in a magnetic moment of Fe_{II} which is larger than that of Fe_I.

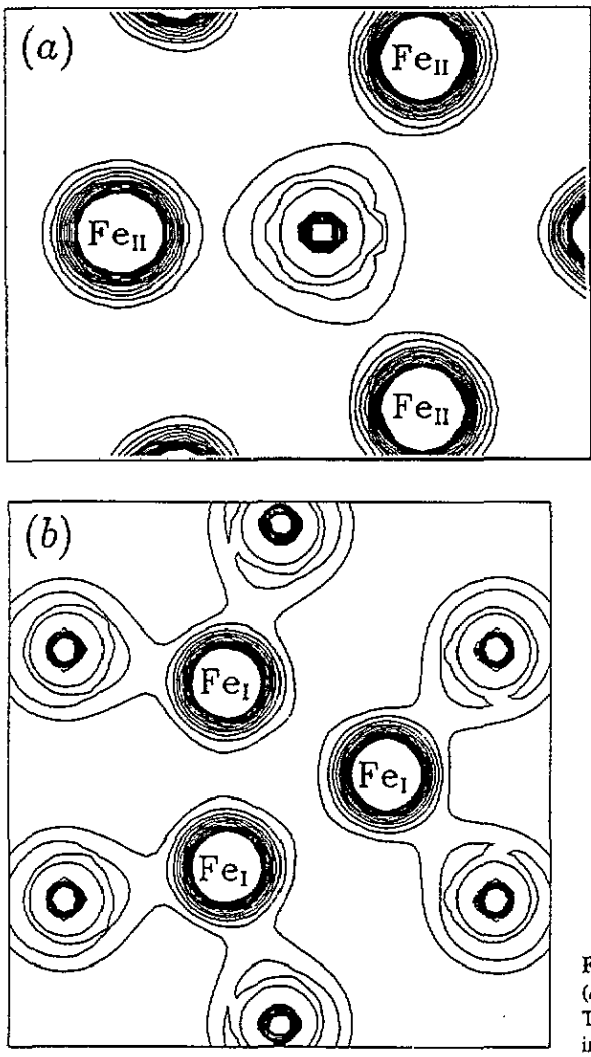

Figure 3. Charge density for the host cluster: (*a*) on the Fe_{II}–P plane; (*b*) on the Fe_I–P plane. The contours are from 0.06 au^{-3} to 0.49 au^{-3} in steps of 0.03 au^{-3}.

As to the mechanism by which P influences the Fe magnetic moment, one can think of the P p states as interacting with Fe d states and forming bonding and antibonding p–d hybrids. Whereas the bonding hybrids lie in the field valence region, the antibonding hybrids lie above the Fermi level. To accommodate the total charge, some charge must

migrate to the antibonding hybrids and, since the Fermi energy is below the latter, the charge is accommodated in the empty states near the Fermi energy, which are mainly minority-spin states. Here it is worth pointing out that the effect of P neighbours is to displace majority-spin electrons to minority-spin states while maintaining the total number of d electrons as nearly constant. So, in Fe_2P, the local magnetic moments for Fe_I and Fe_{II} atoms are very different owing to their different local environments, while the electron occupations are nearly the same for Fe_I and Fe_{II} atoms.

The DOS is a very important quantity for understanding the energy spectrum of valence eigenfunctions. The DOS for the cluster model is obtained by Lorentzian broadening (0.1 eV) of the cluster discrete energy levels to simulate solid state bands. Figures 4(*a*) and 4(*b*) show the local 3d DOSs for Fe_{II} and Fe_I atoms, respectively. There are obvious differences between the local 3d DOSs of Fe_{II} and Fe_I.

(1) The Fe_I 3d DOS has much broader features than the Fe_{II} 3d DOS does, which results from the greater interaction between the Fe_I atom and its environment.

(2) The energy splitting between the main (majority- and minority-spin) 3d peaks is larger for the Fe_{II} site than for the Fe_I site, which shows that the average d–d exchange interaction for Fe_{II} atoms is greater than for the Fe_I atoms.

On the basis of the above discussion, we note that, for Fe_2P, the Fe_I atom bonds with P atoms strongly; its 3d electrons are spatially extended. On the other hand, the Fe_{II} atom is surrounded loosely by P atoms; its 3d electrons are almost localized on the Fe_{II} atom. Therefore, the Fe_{II} magnetic moment is larger than the Fe_I magnetic moment.

3.2. *$(Fe_{1-x}Ni_x)_2P$ compounds*

Above we have studied the electronic structures and magnetic moments of Fe_2P. In this section, we shall investigate the interesting magnetic behaviours of Ni-substituted Fe_2P compounds. Mössbauer experiments on the $(Fe_{1-x}Ni_x)_2P$ system [24] have revealed that Ni atoms occupy the M_I site preferentially in the range $0 \leqslant x < 0.3$, but the M_{II} site for $x > 0.7$. We considered two clusters: one is $Fe_3Fe_3Fe_6Ni_6P_1P_{12}P_2$, and the other $Fe_3Ni_3Fe_6Fe_6P_1P_{12}P_2$. The tetrahedral or pyramidal Fe sites are replaced partly by Ni atoms.

We first examine the effects of Ni occupying tetrahedral sites on the electronic structures and the magnetic moment of pyramidal Fe_{II} atoms. The magnetic moments and electron occupation numbers of cluster atoms are summarized in table 2.

Table 2. Calculated magnetic moments μ_i and electron occupation numbers n_i of various sites with Fe_I atoms of the host cluster replaced by Ni.

Site	Atoms in Cluster	Position	μ_{3d} (μ_B)	μ_{4s+4p} (μ_B)	μ_{total} (μ_B)	n_{3d}	n_{4s}	n_{4p}	n_{3s+3p}
Pyramidal	Fe_3	$z = 0$ (in) Fe_{II}	2.28	0.12	2.40	6.31	0.59	0.65	
Pyramidal	Fe_3	$z = 0$ (mediate)	2.99	0.21	3.20	6.13	0.84	0.89	
Pyramidal	Fe_6	$z = 0$ (out)	3.78	0.55	4.33	6.02	1.23	0.67	
Tetrahedral	Ni_6	$z = \pm\frac{1}{2}$ Ni_I	0.12	0.01	0.13	8.73	0.61	0.71	
	P_1	$z = 0$			−0.08				4.85
	P_{12}	$z = \pm\frac{1}{2}$			−0.20				5.16
	P_2	$z = \pm 1$			0.15				5.06

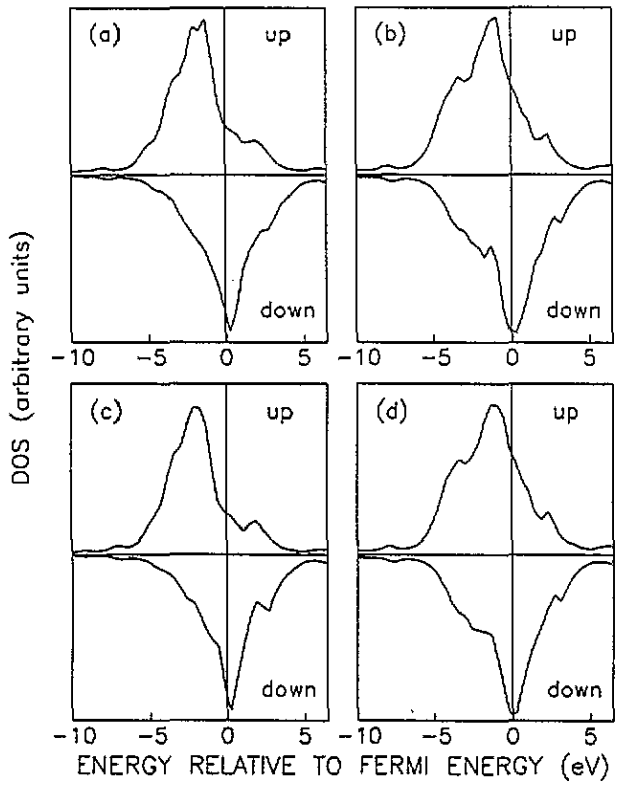

Figure 4. Local 3d DOSS for (*a*) the Fe_{II} site in the cluster $Fe_3Fe_3Fe_6Fe_6P_1P_{12}P_2$, (*b*) the Fe_I site in the cluster $Fe_3Fe_3Fe_6Fe_6P_1P_{12}P_2$, (*c*) the Fe_{II} site with the Ni replacement for Fe_I atoms of the host cluster and (*d*) the Fe_I site with the Ni replacement for Fe_{II} atoms of the host cluster.

From table 2, it may be seen that on comparison with the results of the host cluster $Fe_3Fe_3Fe_6Fe_6P_1P_{12}P_2$ shown in table 1, both Fe_{II} 3d and 4s+4p moments increase slightly, the influence of six Ni_I atoms on the outer Fe atoms is very small, and there is only a very small value for the Ni_I magnetic moment. The magnetization measurements [12] show that the Fe magnetic moment changes little in the range $0 \leqslant x < 0.3$ for the $(Fe_{1-x}Ni_x)_2P$ compounds, since Ni atoms substitute preferentially for Fe_I atoms in this range; this means that substitution of the Ni atom on the tetrahedral Fe site produces little change in the Fe magnetic moment. Our calculated moment is in accord with the experimental value.

In table 2, one can observe that the 3s and 3p electron counts decrease slightly compared with table 1, i.e. Ni substitution for Fe_I atoms results in a small amount of charge transfer from P valence orbitals. As is well known, it is easier for Fe to lose electrons than Ni in an alloy or compound; since M_I sites are surrounded closely by four P neighbours, electrons concentrate more among Ni_I than P atoms than among Fe_{II} and P atoms; thus the influence of P neighbours on Fe_{II} becomes weaker, which leads to a very small value for the Ni_I magnetic moment and an increment in the Fe_{II} moment.

It is worth pointing out that, on the substitution of Ni for the Fe_I site, the value of the central P magnetic moment decreases. As discussed above, p–d mixing results in a reduction in the Fe 3d magnetic moment; in the meantime, it also makes P negatively polarized. Both the decrease in the P magnetic moment and the slight increase in the Fe_{II}

moment mean that the interaction between Fe and P weakens. It is now well recognized that the origin of magnetism can be attributed to intra-atomic and interatomic d–d exchange interactions, that p–d hybridization dilutes the d character of the wavefunction, and that the tendency towards magnetic moment formation and long-range moment coupling is reduced. The reduction in the interaction between Fe and P strengthens the ferromagnetism of $(Fe_{1-x}Ni_x)_2P$ compounds; therefore its Curie temperature is raised, which is in agreement with the experimental result.

The Fe_{II} 3d DOS for Ni occupying Fe_I sites is shown in figure 4(*c*). On comparison with figure 4(*a*), which depicts the Fe_{II} 3d DOS of the host cluster $Fe_3Fe_3Fe_6Fe_6P_1P_{12}P_2$, we can note that, in the case of Ni substitution for Fe_I atoms, the main 3d peak of minority-spin states is becoming sharper, the majority-spin states move downwards and the exchange splitting becomes wider. As a result, the 3d moment of the Fe_{II} atom increases.

Table 3. Calculated magnetic moments μ_i and electron occupation numbers n_i of various sites with Fe_{II} atoms of the host cluster replaced partly by Ni.

Site	Atoms in Cluster	Position	μ_{3d} (μ_B)	μ_{4s+4p} (μ_B)	μ_{total} (μ_B)	n_{3d}	n_{4s}	n_{4p}	n_{3s+3p}
Pyramidal	Fe_3	$z = 0$ (in) Fe_{II}	2.02	0.06	2.08	6.37	0.50	0.79	
Pyramidal	Ni_3	$z = 0$ (mediate)	0.03	0.05	0.08	8.70	0.73	0.77	
Pyramidal	Fe_6	$z = 0$ (out)	3.77	0.56	4.33	6.02	1.11	0.74	
Tetrahedral	Fe_6	$z = \pm\frac{1}{2}$ Fe_I	1.20	0.05	1.25	6.34	0.49	0.87	
	P_1	$z = 0$			−0.23				5.13
	P_{12}	$z = \pm\frac{1}{2}$			−0.18				5.18
	P_2	$z = \pm 1$			−0.27				5.33

Next, we investigate the influence of Fe_{II} atoms partly replaced by Ni on the magnetic moments and the electronic structures of Fe_I sites. In table 3 are displayed the individual atom magnetic moments and electron occupation numbers for the cluster $Fe_3Ni_3Fe_6Fe_6P_1P_{12}P_2$. From this table it is seen that the Fe_I moment is reduced rapidly; there is hardly any change in the magnetic moments of the rest of the Fe_{II} sites, while Ni atoms at pyramidal sites show a negligible moment. The result is consistent with the experimental fact that the magnetic moment per Fe atom decreases with increasing x for $x > 0.3$ since in this range, Ni atoms begin to occupy pyramidal sites partly.

From table 3, one may note that, different from the case of Ni occupying tetrahedral sites, there is little change in the electron occupation numbers with the substitutions of Ni for Fe atoms at pyramidal sites in comparison with the host cluster. In M_2P compounds, the M at the pyramidal sites is loosely surrounded by P neighbours. So it is more difficult for Ni at pyramidal sites to attract the valence electrons of P than for Ni at tetrahedral sites. Accordingly, the interaction between Fe_I and P strengthens relatively when Ni occupies the pyramidal sites, which results in a decrease in the Fe_I magnetic moment.

In table 3, it can be seen that the central P atom magnetic moment increases relative to the case of the host cluster. For the same reasons as above, one can deduce that the interaction between P and Fe strengthens, which results in a reduction in the ferromagnetism of $(Fe_{1-x}Ni_x)_2P$. Therefore the Curie temperature of $(Fe_{1-x}Ni_x)_2P$ compounds is raised in small-x region; then it decreases on further increment in x.

In figure 4(*d*) is drawn the Fe_I 3d DOS for the cluster $Fe_3Ni_3Fe_6Fe_6P_1P_{12}P_2$. On comparison of figure 4(*d*) with figure 4 (*b*) for the Fe_I 3d DOS of host cluster, it can be noted that, with Ni-atom replacement of Fe_{II} sites, there is hardly any change in the

minority-spin state, while the main peak of majority-spin states becomes slightly low and slightly wide; so the empty states of a majority spin increase, which results in a decrease in the Fe_I magnetic moment.

4. Conclusion

We have performed local-spin-density calculations with the DVM for embedded clusters representing Fe_2P and $(Fe_{1-x}Ni_x)_2P$ compounds. The electronic structures and magnetic moments of the distinct Fe sites in Fe_2P have been obtained, and the influence of Ni replacement of Fe_I and Fe_{II} sites on the local magnetic properties of $(Fe_{1-x}Ni_x)_2P$ compounds has been investigated. The following is a summary of our results.

(1) For Fe_2P, the local magnetic moment of Fe_{II} is larger than that of Fe_I owing to the greater hybridization of Fe_I with P, which is in accord with experimental results.

(2) When Ni substitutes on tetrahedral Fe sites, there is a small increment in the Fe_{II} magnetic moment, and the ferromagnetism of $(Fe_{1-x}Ni_x)_2P$ compounds is strengthened, which results from the weakening interaction of Fe_{II} with P. On the contrary, the Fe_I magnetic moment decreases when Ni replaces pyramidal Fe sites.

Acknowledgment

This work was performed on a DEC-5000, at the Institute of Physics, Academia Sinica.

References

[1] Stein F and Dietz G 1989 *J. Magn. Magn. Mater.* **81** 294
[2] Logan J and Yung M 1976 *J. Non-Cryst. Solids* **21** 151
[3] Haughton J L 1927 *J. Iron Steel Inst.* **115** 417
[4] Meyer A J P and Cadeville M C 1962 *J. Phys. Soc. Japan* **17** 223
[5] Fujii H, Hokabe T, Kamigaichi T and Okamoto T 1977 *J. Phys. Soc. Japan* **43** 41
[6] Wäppling R, Häggstrom L, Ericsson T, Devanarayanan S, Karlsson E, Carlsson B and Rundqvist S 1975 *J. Solid State Chem.* **13** 258
[7] Fujii H, Komura S, Takeda T, Okamoto T, Ito Y and Akimitsu J 1979 *J. Phys. Soc. Japan* **46** 1616
[8] Fruchart R, Roger A and Senateur J P 1969 *J. Appl. Phys.* **40** 1250
[9] Fujii H, Hokabe T, Eguchi K, Fujiwara H and Okamoto T 1982 *J. Phys. Soc. Japan* **51** 414
[10] Dolia S N, Krishnamurthy A and Srivastava B K 1988 *J. Phys. C: Solid State Phys.* **21** 6005
[11] Bacmann N, Fruchart D, Chenevier B, Fruchart R, Puertolas J A and Rillo C 1990 *J. Magn. Magn. Mater.* **83** 313
[12] Fujii H, Hokabe T, Fujwara H and Okamoto T 1978 *J. Phys. Soc. Japan* **44** 96
[13] Dolia S N, Krishnamurthy A, Ghose B and Srivastava B K 1993 *J. Phys.: Condens. Matter* **5** 451
[14] Messmer R P 1981 *Phys. Rev.* B **23** 1616
[15] Elzain M E 1991 *Physica* B **173** 251
[16] Guenzburger D and Ellis D E 1985 *Phys. Rev.* B **31** 93
[17] Chacham H, Galvão da Silva E, Guenzburger D and Ellis D E 1987 *Phys. Rev.* B **35** 1602
[18] Press M R, Khanna S N and Jena P 1987 *Phys. Rev.* B **36** 5446
[19] Cai J W, Luo H L, Zeng Z and Zheng Q Q 1993 *J. Phys.: Condens. Matter* **5** 5343
[20] Ellis D E 1968 *Int. J. Quantum Chem. Symp.* **2** 35
Ellis D E and Painter G P 1970 *Phys. Rev.* B **2** 2887
[21] von Barth U and Hedin L 1972 *J. Phys. C: Solid State Phys.* **5** 1629
[22] Press M R, Liu F, Khanna S N and Jena P 1989 *Phys. Rev.* B **40** 399
[23] Carlsson B, Gölin M and Rundqvist S 1973 *J. Solid State Chem.* **8** 57
[24] Maeda Y and Takashima Y 1973 *J. Inorg. Nucl. Chem.* **35** 1963